Contents lists available at ScienceDirect

Food Chemistry

journal homepage: www.elsevier.com/locate/foodchem

Kappa-carrageenan enhances the gelation and structural changes of egg yolk via electrostatic interactions with yolk protein

Min Huang [a,b], Yuzhu Mao [a,b], Hongliang Li [c], Hongshun Yang [a,b,*]

[a] Department of Food Science and Technology, National University of Singapore, 117542, Singapore
[b] National University of Singapore (Suzhou) Research Institute, 377 Lin Quan Street, Suzhou Industrial Park, Suzhou, Jiangsu 215123, PR China
[c] Guangzhou Welbon Biological Technology Co., Ltd, Guangzhou, Guangdong 523660, PR China

ARTICLE INFO

Keywords:
Protein
Polysaccharide
Carrageenan
Rheology
Gelation
Physicochemical property
CLSM
FTIR

ABSTRACT

The effect of κ-carrageenan (κ-C) on yolk over heat-induced gelation at natural yolk pH (6.2) and natural whole egg pH (7.5) was studied. The results showed the zeta potential values changed from -2.3 to -31.3 mV, from -8.6 to -28.6 mV for native pH yolk and pH 7.5 yolk because of the κ-C addition, respectively. These results indicated electrostatic interactions formed between protein and κ-C. The average area of holes formed by yolk gelation increased by κ-C addition. The addition of 1.0% κ-C decreased the gelling points from 62.1 to 54.4 °C, from 64.5 to 61. 6 °C for native pH and pH 7.5 yolk, respectively. A schematic model was established to show that κ-C enhances the yolk properties via electrostatic interactions. And the Fourier transform infrared (FTIR) spectroscopy verified the formation of κ-C-protein interactions. This study provides a guidance for designing novel food systems containing yolk and κ-C.

1. Introduction

Egg yolk, as a source of high quality protein, is widely used in food products such as cakes. It also presents superior functional properties such as emulsifying, coagulating, and gelling (Aguilar, Cordobés, Raymundo, & Guerrero, 2017; Slade, Kweon, & Levine, 2020; Zhang et al., 2019). Considering the composition, egg yolk comprises approximately 50% water, 31–35% lipids, 15–17% proteins, and 1% carbohydrates (Abeyrathne, Lee, & Ahn, 2013; Aguilar et al., 2017). On structural level, yolk is a complex system consisting of aggregates (granules) in suspension in yellow fluid (plasma) with low-density lipoproteins (LDLs) and other proteins (Anton, 2013; Yang et al., 2020).

Kappa-carrageenan (κ-C) is a natural sulphated polysaccharide extracted from red seaweeds and used as thickener, stabilizer, and texturing agent in food industry (Necas & Bartosikova, 2013; Yang, Gao, & Yang, 2020). The gelation of κ-C in aqueous solution involves two steps: the transition from initial random coil to helix structure and the double helices aggregation introduced by mono or double positive ions. The gelation temperature of κ-C can be affected by the types and concentrations of cations, and the strength of the formed gels depends more on the concentration of κ-C and the types and concentrations of cations (Aguilar et al., 2017; Nguyen, Nicolai, Benyahia, & Chassenieux, 2014). However, the gel strength of κ-C can disappear when the pH values are below 5.5 in solutions and below 4.3 for heat-set systems due to autohydrolysis effect (Aguilar et al., 2017).

Previous reports emphasised the importance of protein-polysaccharide interactions in designing novel food formulations (Doublier, Garnier, Renard, & Sanchez, 2000; Lopes-da-Silva & Monteiro, 2019; Wu, Lin, Singh, & Ye, 2020). The main non-covalent interactions between protein and polysaccharide include electrostatic interactions, steric exclusion, hydrophobic interactions, and hydrogen bonding (McClements, 2006). Protein-polysaccharide interactions play a critical role in flow, stability, texture, and mouth feel of food and other macroscopic properties. Furthermore, it can control the interactions between the biopolymers and then provide textural and sensory properties through creating microstructure in food systems (Aguilar et al., 2011). The relative importance of these interactions in a specific system hinges on several elements, including the polymers involved, the liquid mixture composition, and the conditions of the environment (McClements, 2006).

Egg yolk and κ-C are found together in many food products such as mayonnaise (Liu, Xu, & Guo, 2007). Indeed, the effects of κ-C on egg yolk properties were studied in previous literature (Aguilar et al., 2011, 2017). The network formed by heating in yolk/κ-C systems was

* Corresponding author.
E-mail address: fstynghs@nus.edu.sg (H. Yang).

https://doi.org/10.1016/j.foodchem.2021.129972
Received 13 November 2020; Received in revised form 5 April 2021; Accepted 25 April 2021

dominated by protein. Increasing κ-C concentration in yolk enhanced the viscoelastic properties and formed electrostatic interactions of yolk/κ-C dispersions at pH 3.5, 4.5, 5.0, and 6.0 (Aguilar et al., 2017). The exclusion volume effect between protein and polysaccharide macromolecules plays more important role when there is no net charge at protein surfaces (Aguilar et al., 2011). These studies were focused on natural yolk pH or pH values lower than isoelectric point (PI) of yolk (around 5.6). But the pH value of whole egg is in the range of 7.06-8.76 (Dong, Dong, Peng, Tang, & Tang, 2017). Thus, despite all the above developments, the behaviour of yolk/κ-C systems in natural whole egg pH needs to be confirmed. Moreover, the structures of yolk/κ-C systems have not been sufficiently studied.

The main objective of this study was to elucidate the effect of κ-C on the behaviour and structure changes of egg yolk after application of thermal treatment at natural yolk pH (6.2) and natural whole egg pH (7.5). To achieve this objective, the viscosity, strain sweep test, and thermal gelation process of different yolk/κ-C systems was measured by a rheometer. Zeta potential was used to determine the surface charge of all samples. Confocal laser scanning microscope (CLSM) was employed to investigate the structure at the micro level. Finally, the possible mechanism for the effect of κ-C on thermal gelation behaviour of egg yolk was proposed and verified by Fourier transform infrared (FTIR) spectroscopy analysis.

2. Materials and methods

2.1. Materials and sample preparation

The κ-carrageenan (κ-C) powder (molecular weight of 300–400 kDa as reported by the supplier) was procured from Sigma Aldrich (Singapore). Chicken eggs were purchased from a local supermarket (Premium eggs, Fairprice, Singapore). The mineral content was measured via Shimadzu ICPE-9800 Multitype ICP Emission Spectrometer (Shimadzu Corp., Kyoto Japan) according to Takahashi et al. (2016). The mineral content of κ-C was 0.52 ± 0.05 wt% of Ca^{2+}, 2.32 ± 0.03 wt% of Cu^{2+}, 4.33 ± 0.08 wt% of K^{+}, 1.37 ± 0.01 wt% of Na^{+}, and 4.72 ± 0.04 wt% of Zn^{2+}. The mineral content of egg yolk was 0.06 ± 0.00 wt% of Ca^{2+}, 0.04 ± 0.00 wt% of K^{+}, and 0.02 ± 0.00 wt% of Na^{+}. Chicken eggs were hand broken and the egg white was removed carefully by a separator and absorbent paper. The pH values of natural yolk (6.2 ± 0.1) and whole egg (7.5 ± 0.1) were determined by a pH meter (Mettler Toledo, Greisensee, Switzerland). The pH values of yolk were adjusted to the desired whole egg pH values (7.5) using 1 mol/L NaOH (analytical grade, Merck, Germany). The yolk was stirred at 200 rpm for 5 min first and the yolk/κ-C mixtures were prepared by dispersing different amounts of κ-C (0.1, 0.5, and 1.0 wt%) in yolk by several times in small amounts under stirring (200 rpm, 60 min) at room temperature. The solid content of yolk was 48.97 ± 0.28 wt% by measuring the loss of weight after drying 24 h in an oven (105 °C).

2.2. Zeta potential measurement

Zeta potential analysis for all samples was measured using a NanoBrook Omni Zeta potential analyser (Brookhaven Instruments, NY, USA) (Sow, Nicole Chong, Liao, & Yang, 2018). The liquid yolk samples were diluted by 100 times with DI-water and adjusted to desired pH values. The phase analysis light scattering (PALS) mode and the Smoluchowski's model were applied.

2.3. Rheological tests

All samples were left for 30 min at room temperature before the rheological test. Rheological tests were performed using a stress-controlled rheometer (MCR 102, Anton Paar, Graz, Austria), equipped with a Peltier temperature controller. A plate-and-plate geometry (25 mm) with 0.5 mm gap where the samples were equilibrated at 20 °C for 10 min. The steady shear flow test was conducted over shear rate of 0.01 to 100 s^{-1} to obtain flow curves at 20 °C. For oscillation measurements, the edge of the sample was covered with a thin layer of silicone oil to avoid water evaporation. Strain sweep test was conducted from 0.01% to 100% at standard frequency of 1 Hz in order to determine the linear viscoelastic region (LVR) (Takahashi, Kurose, Okazaki, & Osako, 2016). Temperature ramp test was performed from 20 to 90 °C at a rate of 1.5 °C/min and keep at 90 °C for 30 min before decreasing to 20 °C at the same rate (Aguilar et al., 2017).

2.4. CLSM analysis

The fluorescently labelled samples were prepared according to a previous method with slight modifications (Razzak, Kim, & Chung, 2016). Rhodamine B and FITC were used to label yolk protein and κ-C, respectively. The mixture of FITC and rhodamine B dye (0.1 g/L in ethanol) were at a ratio of 1:2. The yolk samples were dissolved in deionized water (6.67%, w/v) and followed by the addition of the dye at a ratio of 1:100 (v/v). Labelling was carried out at room temperature for 30 min. No effect of labelling on the phase separation was observed. Then the samples were smeared on a cover glass slide. The microstructure was captured using an Olympus Fluoview FV1000 confocal scanning unit (Tokyo, Japan) equipped with argon ion and helium–neon (HeNe) lasers. The excitation/emission wavelengths of the FITC and rhodamine B were 490/525 nm and 540/625 nm, respectively. Images were taken at 60 × magnification (PlanApo 60×/1.0 WLSM 0.17) with water immersion for liquid samples and at 10 × magnification for solid samples. The images were processed using Fluoview software (Olympus, Tokyo, Japan) and ImageJ (National Institutes of Health, USA) based on 20 images for each sample.

2.5. Fourier transform infrared (FTIR) spectroscopy analysis

The mixed yolk/κ-C liquids were stored in −80 °C for at least 24 h for further analysis. As for the solid sample, the mixed yolk/κ-C sample was sealed in a container and heated in water bath for 30 min at 90 °C. All samples were stored in −80 °C for at least 24 h and then freeze-dried for 5 days. The spectrum in the range of 4000–600 cm^{-1} was collected with a Spectrum One FTIR spectrometer (PerkinElmer, Waltham, MA, USA) fitted with an ATR infrared cell (zinc selenide crystal) at 4 cm^{-1}

Table 1
Summary of the power law parameters and the average area of holes formed by yolk/κ-C gelation.

Sample	Zeta potential (mV)		*K* (Pa•s^n)		*n*		Average area of holes (μm^2)	
	Native pH (6.2)	pH 7.5	Native pH (6.2)	pH 7.5	Native pH (6.2)	pH 7.5	Native pH (6.2)	pH 7.5
Control	−2.3 ± 0.9 ^{dB}	−8.6 ± 0.7 ^{cA}	0.83 ± 0.02 ^{aA}	5.55 ± 0.32 ^{bB}	0.86 ± 0.01 ^{cB}	0.19 ± 0.01 ^{aA}	1748.6 ± 313.6 ^{aA}	3589.3 ± 746.2 ^{aB}
yolk + 0.1% κ-C	−7.6 ± 0.8 ^{cA}	−10.6 ± 1.8 ^{bcA}	0.71 ± 0.02 ^{aA}	5.09 ± 0.09 ^{bB}	0.86 ± 0.01 ^{cB}	0.22 ± 0.01 ^{aA}	2974.9 ± 555.0 ^{aA}	4598.0 ± 878.0 ^{aA}
yolk + 0.5% κ-C	−23.7 ± 1.2 ^{bA}	−13.6 ± 1.4 ^{bB}	1.14 ± 0.03 ^{bA}	1.93 ± 0.24 ^{aB}	0.80 ± 0.01 ^{bB}	0.19 ± 0.03 ^{aA}	3167.3 ± 783.2 ^{aA}	8483.0 ± 1962.3 ^{abB}
yolk + 1.0% κ-C	−31.3 ± 4.0 ^{aA}	−28.6 ± 2.2 ^{aA}	1.99 ± 0.14 ^{cA}	12.48 ± 0.47 ^{cB}	0.75 ± 0.02 ^{aB}	0.33 ± 0.01 ^{bA}	6703.0 ± 1721.6 ^{bA}	13042.2 ± 6684.1 ^{bA}

*κ-C means κ-carrageenan. Values are mean with standard deviation. Values with different superscripts in lowercase alphabets in the same column are significantly different among different κ-C concentration ($P < 0.05$). Values with different superscripts in uppercase alphabets in the same row are significantly different across different pH ($P < 0.05$).

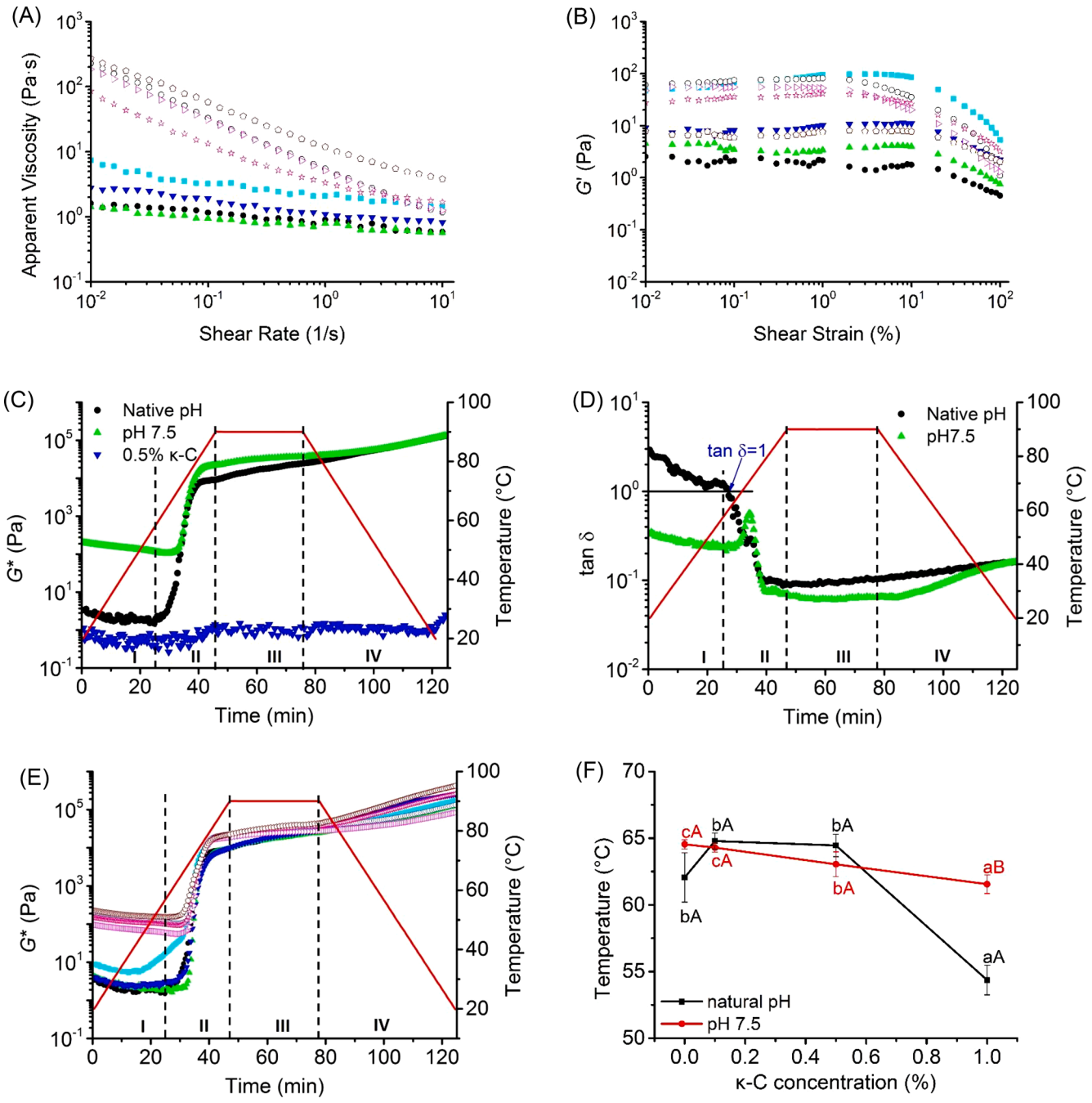

Fig. 1. Evolution of the apparent viscosity, strain sweep, and the complex modulus G^* and tan δ during the thermal cycle. (A) The dependence of the apparent viscosity on the shear rate of different yolk/κ-C systems; (B) Effect of strain on the storage modulus (G') of different yolk/κ-C systems; (C) The G^* of native pH yolk, pH 7.5 yolk, and 0.5% κ-C; (D) The values of tan δ for native pH yolk, pH 7.5 yolk; (E) The G^* of different yolk/κ-C systems; (F) The effect of κ-C concentration on gelling point of yolk samples.●, native pH yolk; ▲, native pH yolk + 0.1% κ-C; ▼, native pH yolk + 0.5% κ-C;■, native pH yolk + 1.0% κ-C;○, pH 7.5 yolk;◁, pH 7.5 yolk + 0.1% κ-C; ☆, pH 7.5 yolk + 0.5% κ-C; ⬠, pH 7.5 yolk + 1.0% κ-C.

resolution for 32 scans. The FTIR spectra were processed by the Omnic software 8.2 (Thermo Fisher Scientific Inc. Waltham, MA, USA). The yolk protein spectra were studied to provide complementary information by deconvolution at the amide I band (1700–1600 cm^{-1}). The bandwidth was set at 30 cm^{-1} and the enhancement factor was 1.3. According to Byler and Susi (1986), gaussian peak fitting was conducted on the deconvolved spectra in the OriginPro 9.0 software. The relative integrated areas of the corresponding fitted peaks were used to calculate the relative percentages of the secondary structures of protein.

2.6. Statistical analyses

All tests were carried out in triplicates and results are reported as the mean and standard derivation of these measurements. Statistical analysis was performed using ANOVA followed by a Student-Newman-Keuls (SNK) procedure as implemented in the SPSS (IBM Corp., Armonk, NY, USA), or using the one-way analysis of variance as implemented in the statistical software MS office Excel 2020 (Microsoft, Redmond, WA, USA). The P values that were<0.05 were considered statistically significant.

3. Results and discussion

3.1. Zeta potential of yolk/κ-C samples

The particle charge of yolk in different systems was examined (Table 1). First, the isoelectric point of egg yolk is between 5 and 6 (Aguilar et al., 2017; Navidghasemizad, Temelli, & Wu, 2015), and the zeta potential of yolk at native pH was slightly negative (-2.32 mV). Changing the pH value to 7.5 increased the negative charge of yolk to -8.58 mV. Many -COO- groups exposed when pH was higher than pI (Causeret, Matringe, & Lorient, 1991). The zeta potential of κ-C was around −57.1 mV, which is strong negatively charged and consisting with previous report (Sow et al., 2018). In the yolk/κ-C samples, the zeta potential values were all between pure yolk samples and pure κ-C samples in both pH systems (Table 1). As reported, the sulphated polysaccharides such as carrageenan have the ability to interact with proteins above their isoelectric points (Samant, Singhal, Kulkarni, & Rege, 1993). κ-C contains sulphate group (-OSO_3-), which could bind the amino group (-NH_3^+) of proteins through electrostatic interactions (Doublier et al., 2000; Navidghasemizad et al., 2015). The electrostatic interactions formed by sulphate group (-OSO_3-) and protein are stronger than those formed by carboxylic group (–COO^-) and protein (Doublier et al., 2000). This indicated that the positive charge groups of yolk proteins bound with κ-C.

3.2. Viscosity of different yolk/κ-C samples

Fig. 1A shows the dependence of the apparent viscosity with the shear rate of samples from different egg yolk/κ-C systems. Overall, samples at pH 7.5 had higher viscosity than those at native pH. All samples showed shear-thinning behaviour because the apparent viscosity decreased with the shear rate, although the decline slopes of yolk at native pH are very small. Similar behaviour has been reported by other researchers (Severa, Nedomová, & Buchar, 2010).

The experimental data in Fig. 1A could be described by the power-law equation as follow:

$$\eta = K \cdot \dot{\gamma}^{n-1}$$

where η is the apparent viscosity (Pa•s), K is consistency coefficient (Pa•s^n), $\dot{\gamma}$ is shear rate (s^{-1}), and n is flow behaviour index. The related power law parameters are shown in Table 1.

Consistency coefficient K indicates the consistency of the system. Samples at pH 7.5 showed higher K values than the corresponding samples at native pH. As for the influence of κ-C, the addition of κ-C increased the K values significantly at native pH, indicating the increase of consistency of the system. At pH 7.5, the 0.1% κ-C addition did not

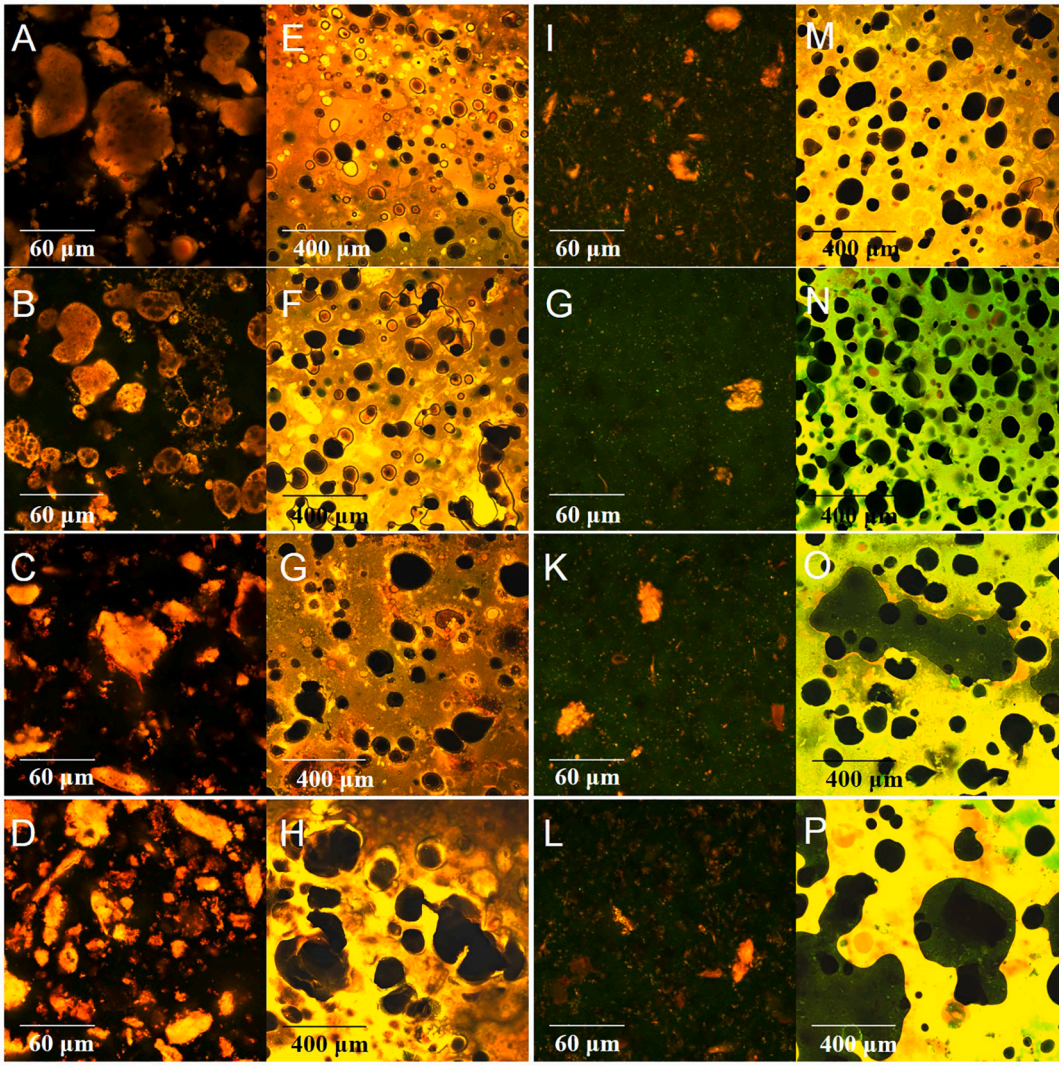

Fig. 2. Microstructure of the samples at native pH (A-H) and at pH 7.5 (I-P) with the addition of κ-C at 0.0% (A, E, I, M), 0.1% (B, F, G, H), 0.5% (C, G, K, O), and 1.0% (D, H, L, P) concentrations before heating (A-D, I-L) and after heating (E-H, M−P).

change the consistency of the system when comparing with the control sample. However, the 0.5% κ-C addition decreased the *K* value significantly while the 1.0% κ-C addition increased it, suggesting κ-C had a more complex effect on yolk at pH 7.5 condition. Flow behaviour index *n* reflects the degree of change in viscosity as the shear rate changes. The results showed that samples at pH 7.5 had lower *n* values than samples at native pH, indicating that yolk samples at pH 7.5 showed a more remarkable non-Newtonian behaviour. As for the influence of κ-C, at native pH, the addition of κ-C decreased the *n* values significantly, indicating relatively faster decay of the apparent viscosity with the shear rate. At pH 7.5, the κ-C addition increased the *n* values significantly only at 1.0% concentration in the yolk/κ-C systems.

Previous study proves that at pH > 6.3 (native pH), the yolk granules are destructed because of electrostatic repulsions and induce higher viscosity (Causeret et al., 1991). Thus, the yolk at pH 7.5 became more viscous and more distinct shear-thinning behaviour than that of native pH. As a kind of anionic sulphate polysaccharide, κ-C has the ability to react with cationic groups (Necas & Bartosikova, 2013). Thus, we speculated that the addition of κ-C in yolk system can cause imbalance in protein–protein interactions and form protein-polysaccharide interactions, resulting in the changes of viscosity.

3.3. Strain sweep analysis of different yolk/κ-C samples

Fig. 1B presents the effects of strain amplitude on the storage modulus (G') of different yolk/κ-C systems. The native pH yolk performed the lowest G' values. The G' values were almost constant in the LVR, and a decrease of G' was caused by further increasing the applied stress due to the breaking of protein–protein interactions. With the increase of κ-C concentration, the G' values of native pH yolk/κ-C systems increased significantly, indicating that the κ-C addition made the yolk sample have a stronger structure with higher resistance to applied stress. The G' values of yolk at pH 7.5 were higher than the native pH yolk, suggesting the pH 7.5 yolk had higher resistance to applied stress since the destructed yolk granules formed new interactions. Increasing the concentration of κ-C led to decreased G' values at pH 7.5, which was different with samples at native pH. It was easier for the negative-charged κ-C to interact with positive charge groups in protein when the yolk granules were destructed at pH 7.5 (>pI). The formation of hydrogen bond between functional groups of proteins and water was disturbed easily and then lowered the G' values (Liu, Bao, Xi, & Miao, 2014; Navidghasemizad, Temelli, & Wu, 2014).

3.4. CLSM analysis of different yolk/κ-C samples

The microstructures of different yolk/κ-C systems were investigated by CLSM (Fig. 2), the green and red fluorescence intensity is summarised in Table A1, and the images of pure κ-C are shown in Fig. A1. The green dots in all liquid samples and green domain in all solid samples should be the dyed κ-C. Many granules and spheres were observed in natural pH yolk before heating (Fig. 2A). These structures should be the main components of yolk protein: aggregates (granules) and low-density lipoproteins (LDL). However, big granules cannot be found in pH 7.5 yolk (Fig. 2I), indicating these granules were disorganized because of the pH increase. When increasing the κ-C concentration, the granules became smaller and also disorganized, suggesting the negative-charged κ-C disturbed the aggregation of proteins. After heating, the yolk suspension at native pH formed a network with many small holes because of the gelation of the protein (Kiosseoglou, 2003). The average area of these holes was shown in Table 1. Comparing with the native pH yolk, the holes formed by yolk at pH 7.5 became larger significantly. The addition of κ-C also increased the average area of holes significantly. This indicated that the interaction formed by yolk protein and κ-C influenced the structures of sample during heating. The κ-C maybe insert into the denatured protein matrix and then affect the thermal gelation process.

3.5. The thermal gelation process of different yolk/κ-C samples

3.5.1. Effect of pH on thermal gelation of yolk

Fig. 1C shows the values of complex modulus (G^*) over a thermal cycle for the 0.5% κ-C solution, yolk at native pH, and yolk at pH 7.5. Four stages can be found in the thermal behaviour of yolk at native pH as labelled. Stage I: Gel development period as no protein denaturation occurred but only thermal-induced increased mobility occurred with

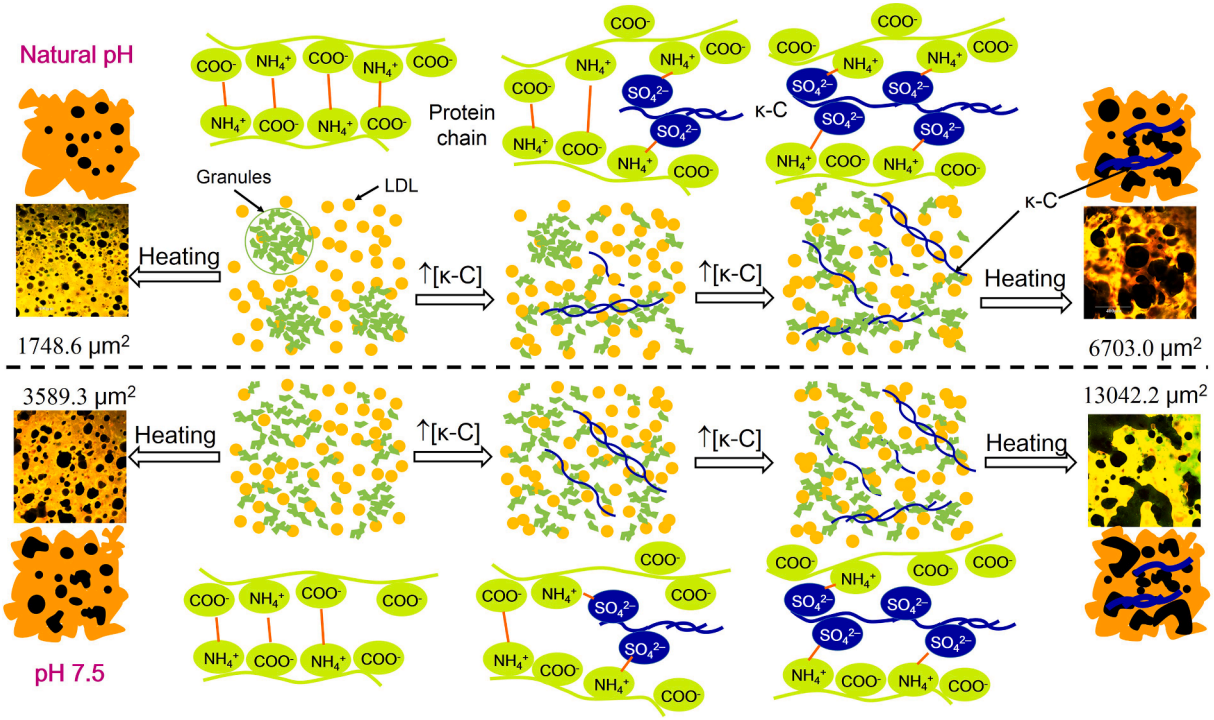

Fig. 3. Schematic model illustrating the effect of κ-C addition on the yolk structure in different systems.

temperature increasing. The G^* values were low and had a slight decrease. Stage II: The G^* values increased sharply because of the thermal induced protein denaturation, as well as the aggregation of partially denatured protein molecules and random association of the aggregates to form a protein gel network. Stage III: A tendency to a plateau value in G^* values occurred in this isothermal stage. Stage IV: A noticeable reinforcement of the gel network took place in this cooling stage. These stages were also verified in previous studies (Aguilar et al., 2017; Zhang et al., 2019).

As for the yolk at pH 7.5, this four stages were still obvious during the thermal cycle (Fig. 1C). The G^* values were much higher than those of yolk at native pH at stage I, II, and III, and then became similar with yolk at native pH in the cooling period, in line with previous study (Aguilar et al., 2017).

The behaviour of κ-C solution over the thermal cycle is shown in Fig. 1C and is completely different. Overall, the κ-C solution shows very low viscoelastic properties during the whole test. A slight decrease could be observed in stage I and the beginning of stage II because of the heating process. At the end of stage II, a moderate increase occurred in G^* values resulting from the hydration of κ-C. The G^* values remain stable afterwards until an increase appear at the end of stage IV, where the κ-C forms a gel since temperature is reduced (Aguilar et al., 2017).

Fig. 1D shows the loss factor tan δ (tan $\delta = G''/G'$). The values of tan $\delta < 1$ reflect a predominance of the storage modulus (G') versus the loss modulus (G'') (solid-like behaviour), while tan $\delta > 1$ denotes a predominance of G'' versus G' (liquid-like behaviour). For yolk at native pH, the values of tan δ decreased from>1 to<1 as temperature increasing. The crossover point (when tan $\delta = 1$) indicated the behaviour of yolk changing from liquid-like to solid-like due to heating process in stage I. This point was usually considered as the gelling point (Cordobés, Partal, & Guerrero, 2004; Zhang et al., 2019). However, for yolk at pH 7.5, the values of tan δ were always lower than 1 although a peak can be observed for tan δ values in stage II, suggesting solid-like behaviour was predominant throughout the heating process.

There are many yolk spheres in egg yolk and these spheres are sensitive for both pH and temperature (Anton, 2013; Woodward & Cotterill, 1987). As temperature increased, yolk spheres became a molten state but no denaturation occurred. These changes resulted in the behaviour changes of yolk at natural pH before denaturation. However, the yolk presented higher gel formation ability at pH 7.5 (Fig. 1C). The yolk granules can be destructed due to electrostatic repulsions at pH 7.5 and presented as solid-like behaviour before heating. Only when denaturation occurred in stage II that formed a peak in tan δ values. The gel strength of yolk at different pH after cooling were similar with each other, suggesting changing yolk pH values from native pH (6.2) to the whole egg pH (7.5) did not influence the gel formation significantly after cooling.

3.5.2. *Effect of κ-C on thermal gelation process of different yolk/κ-C systems*

Temperature sweep curves of samples with different κ-C concentrations are shown in Fig. 1E. As can be seen, all samples showed the similar stages as the yolk at native pH had. For yolk/κ-C systems at native pH, 1.0% κ-C exhibited a shorter gel development period and the G^* values

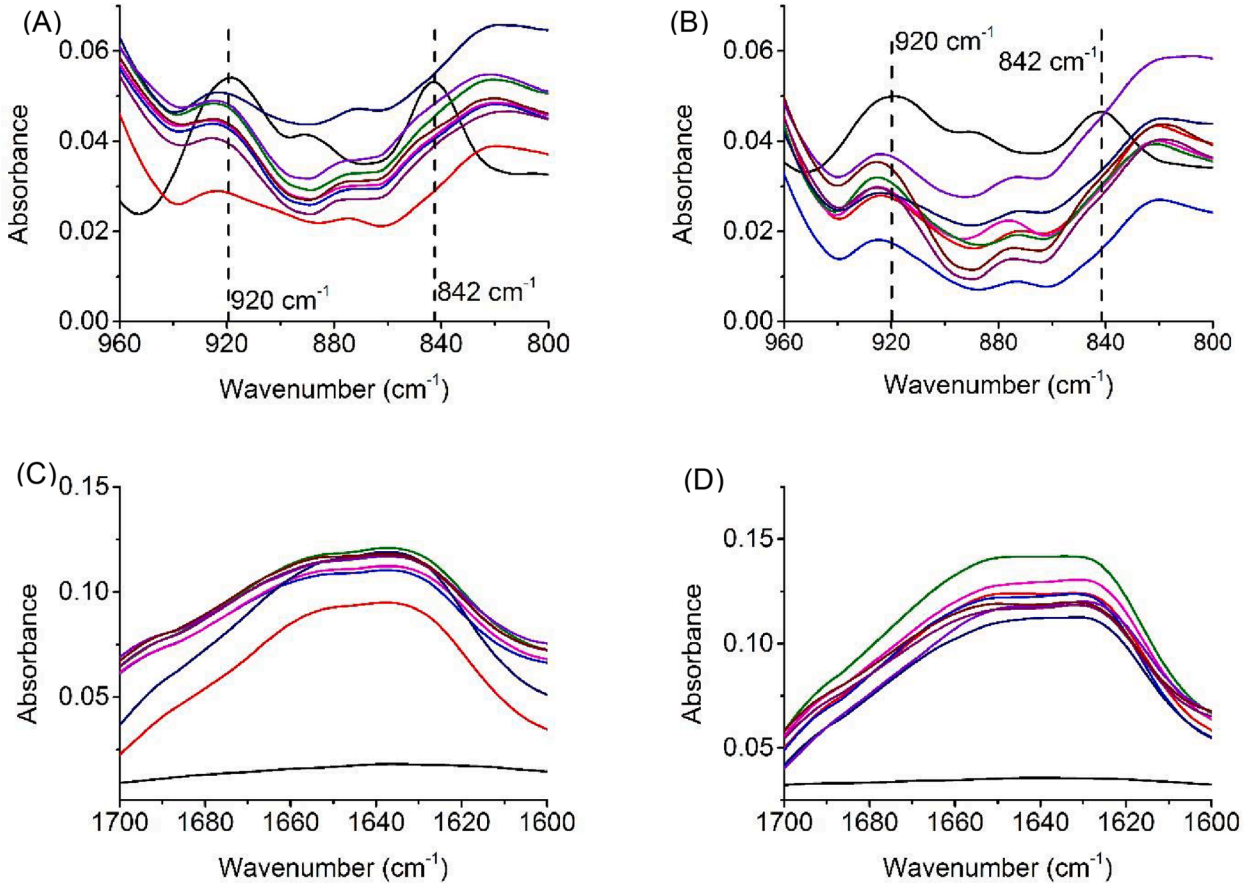

Fig. 4. Infrared spectra of different yolk/κ-C systems. (A) Spectra of liquid yolk/κ-C mixtures in the region of 960–800 cm^{-1}; (B) Spectra of yolk/κ-C mixtures after heating in the region of 960–800 cm^{-1}; (C) Spectra of liquid yolk/κ-C mixtures in the amide I region; (D) Spectra of yolk/κ-C mixtures after heating in the amide I region. Black line: κ-C, red line: native pH yolk, blue line: native pH yolk + 0.1%κ-C, magenta line: native pH yolk + 0.5%κ-C, olive line: native pH yolk + 1.0%κ-C, navy line: pH 7.5 yolk, violet line: pH 7.5 yolk + 0.1%κ-C, purple line: pH 7.5 yolk + 0.5%κ-C, wine line: pH 7.5 yolk + 1.0%κ-C. (For interpretation of the references to colour in this figure legend, the reader is referred to the web version of this article.)

increased, which corresponding to the denaturation of yolk protein. In the cooling period, the addition of 0.5% and 1.0% κ-C presented larger G^* values, suggesting they had greater gel strength than the yolk at native pH. For yolk/κ-C systems at pH 7.5, the addition of 0.1% κ-C decreased the initial G^* values in stage I. During the cooling stage, the yolk sample with 1.0% κ-C showed the largest G^* values when comparing with other samples, indicating the highest gel strength.

To further comparison of the effect of κ-C, the gelling points of yolk in different systems are summarised in Fig. 1F. For yolk at natural pH, the gelling points were the crossover of G' and G'' ($\tan\delta = 1$). Since there was no crossover in yolk at pH 7.5, the gelling points were considered as the temperature where just before G' rapidly increasing (data not shown) (Gunasekaran & Ak, 2000; Zhang et al., 2019).

At native pH, the addition of 0.1% and 0.5% κ-C did not influence the gelling point significantly but 1.0% κ-C addition decreased it. Heating process causes the exposure of hydrophobic groups, leading to hydrophobic aggregation and the formation of a gel (Petruccelli & Anon, 1995; Zhang et al., 2019). The κ-C addition had a moderating effect on the interactions among protein segments. The negative-charged κ-C may interact with positive-charged residues of yolk proteins at native pH, resulting in more exposure of hydrophobic groups, then promoted protein aggregation and had lower gelling points. At pH 7.5 systems, the 0.1% κ-C addition did not change the gelling point significantly while the 0.5% and 1.0% κ-C addition decreased it significantly. Granules are linked by phosphocalcic bridges, which have efficient protection for heat gelation (Anton, 2013). The yolk granules were destructed due to electrostatic repulsions at pH 7.5 (>pI). Then it was easier for the negative-charged κ-C to interact with positive charge groups in protein, promoting the protein aggregation (gel formation).

3.6. Proposed interactions of the effects of κ-C on egg yolk

Based on the results of zeta potential, viscosity, microstructure, and thermal gelation, a schematic model was proposed in Fig. 3 to demonstrate the effect of κ-C on yolk at both native pH and natural whole egg pH (7.5). The native pH yolk was a complex system consisting of protein granules and LDL in yellow fluid (Anton, 2013; Zhou, Hu, Wang, Xue, & Luo, 2016). Heating process could lead to protein denaturation and form a network structure with many small holes. Previous studies reported that polysaccharides such as λ-carrageenan and xanthan gum were used to selective separate proteins from complex systems such as egg yolk since the electrostatic attraction between oppositely charged biopolymers can cause phase separation (Aguilar et al., 2011; Navidghasemizad et al., 2015; Nguyen et al., 2014). Thus, in this study, the addition of κ-C disturbed the aggregation of protein and was thought to form new electrostatic interactions with the protein (Fig. 2, Table 1), leading to the changes of viscosity (Fig. 1A) and the lower gelling points (Fig. 1F). As a result, the formed gel structure had much larger holes (Fig. 2 & Table 1). As for samples at pH 7.5, the yolk granules were destructed (Fig. 2) due to electrostatic repulsions when pH > pI, which lead to the viscosity change when comparing with those of yolk at native pH (Table 1). The addition of κ-C can also disturb the protein aggregation at pH 7.5 and formed electrostatic interactions, resulting in the changes of viscosity and the decrease of gelling point (Fig. 1F). The formed gel had much bigger holes because of the denaturation of aggregated protein and the interactions of yolk protein and κ-C (Fig. 2 & Table 1).

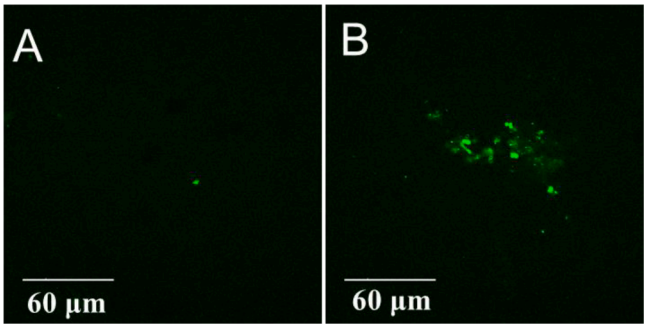

Fig. A1. CLSM images of 0.5% κ-C before heating (A) and after heating (B).

3.7. Validation of the proposed model

FTIR analysis was conducted in order to confirm the proposed schematic diagram. Fig. 4 shows the spectra of all samples in the region of 960–800 cm^{-1}, as well as the amide I region (1700–1600 cm^{-1}). The spectra show strong band at approximately 842 cm^{-1} and 920 cm^{-1}, which are assigned to D-galactose-4-sulfphate and 3,6-anhydro-D-galactose, respectively. These two band are the characteristic signals for κ-C (Gómez-Ordóñez & Rupérez, 2011; Pereira, Sousa, Coelho, Amado, & Ribeiro-Claro, 2003). In yolk/κ-C samples at different pH, these two band cannot be observed (Fig. 4A, 4B), indicating these groups of κ-C disappeared through binding with yolk proteins.

To further understand the changes of yolk protein structure, the percentage of secondary structures were calculated and showed in Table 2. Typically, amide I (1700 ~ 1600 cm^{-1}) is more commonly used as a quantitative method for the secondary structures of proteins because of its stronger peak intensity (Carbonaro & Nucara, 2010; Lin, Tay, Yang, Yang, & Li, 2017). Therefore, the amide I regions of all yolk samples were chosen and deconvolved to calculate the secondary structures and explain the nanostructure changes of yolk protein. Specifically, the components located at 1624, 1650, and 1680 cm^{-1} represent intermolecular β-sheets, α-helix/unordered structures, and β-sheets, respectively (Blume, Dietrich, Lilienthal, Ternes, & Drotleff, 2015; Carbonaro & Nucara, 2010; Guerrero, Kerry, & de la Caba, 2014). In the

Table 2
The percentages of the curve fitting of amide I region for different yolk/κ-C systems.

Sample	Native pH (6.2)			pH 7.5		
	1624 cm^{-1}	1650 cm^{-1}	1680 cm^{-1}	1624 cm^{-1}	1650 cm^{-1}	1680 cm^{-1}
Liquid mixture (before heating)						
Control	23.85 ± 0.74 ^{aA}	54.47 ± 2.29 ^{aA}	21.68 ± 2.83 ^{bA}	24.31 ± 1.01 ^{aA}	53.03 ± 1.59 ^{aA}	22.66 ± 2.57 ^{bA}
yolk + 0.1% κ-C	27.85 ± 0.72 ^{bA}	56.58 ± 1.27 ^{aA}	15.57 ± 1.95 ^{aA}	28.68 ± 0.62 ^{bA}	57.92 ± 1.87 ^{bA}	13.40 ± 1.68 ^{aA}
yolk + 0.5% κ-C	28.84 ± 0.57 ^{bA}	58.53 ± 1.30 ^{aA}	12.63 ± 1.76 ^{aA}	28.88 ± 0.98 ^{bA}	56.09 ± 0.91 ^{bA}	15.03 ± 1.16 ^{aA}
yolk + 1.0% κ-C	27.86 ± 1.09 ^{bA}	58.33 ± 1.82 ^{aA}	13.81 ± 2.39 ^{aA}	29.20 ± 1.82 ^{bA}	57.97 ± 2.08 ^{bA}	12.83 ± 1.76 ^{aA}
Solid mixture (after heating)						
Control	24.76 ± 0.56 ^{aB}	49.50 ± 0.77 ^{cB}	25.74 ± 1.03 ^{aA}	21.48 ± 1.07 ^{aA}	40.63 ± 1.89 ^{aA}	37.89 ± 2.24 ^{cB}
yolk + 0.1% κ-C	24.51 ± 0.71 ^{aB}	37.43 ± 0.79 ^{bA}	38.06 ± 1.47 ^{bB}	22.80 ± 0.52 ^{bA}	50.87 ± 1.24 ^{bB}	26.32 ± 1.76 ^{bA}
yolk + 0.5% κ-C	23.30 ± 0.31 ^{aA}	35.87 ± 0.81 ^{abA}	40.83 ± 1.06 ^{cB}	26.08 ± 0.13 ^{cB}	51.74 ± 2.51 ^{bB}	22.17 ± 2.57 ^{aA}
yolk + 1.0% κ-C	23.41 ± 0.76 ^{aA}	34.88 ± 0.97 ^{aA}	41.71 ± 1.66 ^{cB}	26.63 ± 0.44 ^{cB}	54.24 ± 1.88 ^{bB}	19.13 ± 1.73 ^{aA}

*κ-C means κ-carrageenan. Values are mean with standard deviation. Values with different superscripts in lowercase alphabets in the same column are significantly different among different κ-C concentration ($P < 0.05$). Values with different superscripts in uppercase alphabets in the same row are significantly different across different pH ($P < 0.05$).

Table A1
The fluorescence intensity of different yolk/κ-C systems.

Sample	Natural pH (6.2)		pH 7.5	
	Green fluorescence	Red fluorescence	Green fluorescence	Red fluorescence
Liquid mixture (before heating)				
Control	227.6 ± 18.3 [a]	1603.2 ± 212.4 [a]	238.1 ± 14.8 [a]	1797.8 ± 382.3 [a]
yolk + 0.1% κ-C	236.6 ± 8.1 [a]	1558.1 ± 56.9 [a]	397.8 ± 27.1[b]	1678.2 ± 175.7 [a]
yolk + 0.5% κ-C	244.3 ± 15.4 [a]	1869.5 ± 102.3 [a]	479.6 ± 45.1 [bc]	1438.7 ± 208.9 [a]
yolk + 1.0% κ-C	262.0 ± 16.2 [a]	1645.4 ± 93.5 [a]	549.1 ± 68.1[c]	1397.6 ± 120.7 [a]
Solid mixture (after heating)				
Control	1709.3 ± 375.6 [a]	2818.9 ± 381.6 [a]	2220.7 ± 310.1 [a]	3067.9 ± 366.2 [a]
yolk + 0.1% κ-C	1803.0 ± 343.5 [a]	2911.8 ± 339.2 [a]	2883.7 ± 239.7[b]	2444.2 ± 439.3 [a]
yolk + 0.5% κ-C	1832.3 ± 252.2 [a]	2801.9 ± 315.7 [a]	2949.3 ± 265.7[b]	2741.8 ± 398.7 [a]
yolk + 1.0% κ-C	2008.3 ± 441.2 [a]	2892.1 ± 326.2 [a]	2962.5 ± 213.7[b]	2914.5 ± 363.5 [a]

*κ-C means κ-carrageenan. Values are mean with standard deviation. Values with different superscripts in the same column are significantly different among different κ-C concentration ($P < 0.05$).

liquid samples before heating, the percentages of band at 1624 cm^{-1} increased while those of band at 1680 cm^{-1} decreased significantly upon increasing the κ-C at both pH values. The increasing of intermolecular β-sheets lead to the view that the protein aggregation occurred (Guerrero et al., 2014). Thus, the formation of κ-C and yolk protein interactions disordered the aggregation of yolk proteins and led to the changes in zeta potential, viscosity, gelation, and the CLSM images.

After heating, the secondary structures of yolk protein had significant difference at different pH values. The band at 1624 cm^{-1} and 1650 cm^{-1} decreased while the band at 1680 cm^{-1} increased in yolk protein at pH 7.5 after heating when comparing with the native pH yolk protein. This suggested that the interactions of yolk proteins changed from residual regular structures (e.g. α-helix and unordered structures) into β-sheets when heating at pH 7.5. The κ-C addition had different influence on the yolk protein structures when heated at different pH. At native pH, the percentage of 1650 cm^{-1} band decreased while the percentage of 1680 cm^{-1} band increased when comparing with the control sample due to the addition of κ-C. The κ-C addition might induce structural modification of yolk protein by increasing the β-sheet structure that presented a large surface area for association. This result is similar to the fish gelatin-κ-C complex reported by Sow et al. (2018). However, at pH 7.5, both of the band at 1624 cm^{-1} and 1650 cm^{-1} increased while the band at 1680 cm^{-1} decreased, indicating the β-sheets converted partly into intermolecular β-sheets (hydrogen-bonded antiparallel β-sheets) and α-helix. Extended antiparallel β-sheets are usually found in aggregated proteins, especially in heat-denatured proteins (Guerrero et al., 2014). The κ-C addition concluded the aggregated proteins during heating. This further supported the changes in gelation properties of different yolk/κ-C systems.

4. Conclusions

The zeta potential values changed from -2.3 to -31.3 mV, from -8.6 to -28.6 mV due to the addition of κ-C for the native pH yolk and pH 7.5 yolk, respectively. This indicated that the electrostatic interactions between protein and κ-C formed. The microstructures of yolk/κ-C systems were investigated by CLSM. Increasing pH values and the addition of κ-C both increased the average area of holes significantly formed by yolk gelation. The viscosity and G^* values of pH 7.5 yolk samples were higher than those of native pH yolk samples. Increasing κ-C concentration led to the enhancement of gel formation after heating. The addition of 1.0% κ-C decreased the gelling points from 62.1 to 54.4 °C, from 64.5 to 61.6 °C for the native pH yolk and pH 7.5 yolk, respectively. A schematic model was established to show that κ-C enhances the yolk properties via electrostatic interactions. The results of FTIR analysis confirmed the interactions between yolk protein and κ-C. This study showed the behaviour of yolk and yolk/κ-C in natural yolk pH and natural whole egg pH and provided guidance for designing novel food systems containing yolk and κ-C.

CRediT authorship contribution statement

Min Huang: Conceptualization, Methodology, Investigation, Software, Visualization, Writing - original draft. **Yuzhu Mao:** Methodology, Software, Validation. **Hongliang Li:** Funding acquisition. **Hongshun Yang:** Conceptualization, Funding acquisition, Project administration, Supervision, Writing - review & editing.

Declaration of Competing Interest

The authors declare that they have no known competing financial interests or personal relationships that could have appeared to influence the work reported in this paper.

Acknowledgements

This work was financially supported by the Singapore NRF Industry IHL Partnership Grant (R-143-000-653-281), student support (R-160-002-653-281) and an industry project from Guangzhou Welbon Biological Technology Co., Ltd (R-2017-H-002).

References

Abeyrathne, E. D. N. S., Lee, H. Y., & Ahn, D. U. (2013). Egg white proteins and their potential use in food processing or as nutraceutical and pharmaceutical agents-a review. *Poultry Science, 92*(12), 3292–3299.
Aguilar, J. M., Batista, A. P., Nunes, M. C., Cordobés, F., Raymundo, A., & Guerrero, A. (2011). From egg yolk/κ-carrageenan dispersions to gel systems: linear viscoelasticity and texture analysis. *Food Hydrocolloids, 25*(4), 654–658.
Aguilar, J. M., Cordobés, F., Raymundo, A., & Guerrero, A. (2017). Thermal gelation of mixed egg yolk/kappa-carrageenan dispersions. *Carbohydrate Polymers, 161*, 172–180.
Anton, M. (2013). Egg yolk: Structures, functionalities and processes. *Journal of the Science of Food and Agriculture, 93*(12), 2871–2880.
Blume, K., Dietrich, K., Lilienthal, S., Ternes, W., & Drotleff, A. M. (2015). Exploring the relationship between protein secondary structures, temperature-dependent viscosities, and technological treatments in egg yolk and LDL by FTIR and rheology. *Food Chemistry, 173*, 584–593.
Byler, D. M., & Susi, H. (1986). Examination of the secondary structure of proteins by deconvolved FTIR spectra. *Biopolymers, 25*(3), 469–487.
Carbonaro, M., & Nucara, A. (2010). Secondary structure of food proteins by Fourier transform spectroscopy in the mid-infrared region. *Amino Acids, 38*(3), 679–690.
Causeret, D., Matringe, E., & Lorient, D. (1991). Ionic strength and pH effects on composition and microstructure of yolk granules. *Journal of Food Science, 56*(6), 1532–1536.
Cordobés, F., Partal, P., & Guerrero, A. (2004). Rheology and microstructure of heat-induced egg yolk gels. *Rheologica Acta, 43*(2), 184–195.
Dong, X., Dong, J., Peng, Y., Tang, X., & Tang, X. (2017). Comparative study of albumen pH and whole egg pH for the evaluation of egg freshness. *Spectroscopy Letters, 50*(9), 463–469.
Doublier, J.-L., Garnier, C., Renard, D., & Sanchez, C. (2000). Protein–polysaccharide interactions. *Current Opinion in Colloid & Interface Science, 5*(3-4), 202–214.
Gómez-Ordóñez, E., & Rupérez, P. (2011). FTIR-ATR spectroscopy as a tool for polysaccharide identification in edible brown and red seaweeds. *Food Hydrocolloids, 25*(6), 1514–1520.

Guerrero, P., Kerry, J. P., & de la Caba, K. (2014). FTIR characterization of protein–polysaccharide interactions in extruded blends. *Carbohydrate Polymers, 111*, 598–605.
Gunasekaran, S., & Ak, M. M. (2000). Dynamic oscillatory shear testing of foods-selected applications. *Trends in Food Science & Technology, 11*(3), 115–127.
Kiosseoglou, V. (2003). Egg yolk protein gels and emulsions. *Current Opinion in Colloid & Interface Science, 8*(4-5), 365–370.
Lin, M., Tay, S. H., Yang, H., Yang, B., & Li, H. (2017). Replacement of eggs with soybean protein isolates and polysaccharides to prepare yellow cakes suitable for vegetarians. *Food Chemistry, 229*, 663–673.
Liu, Q., Bao, H., Xi, C., & Miao, H. (2014). Rheological characterization of tuna myofibrillar protein in linear and nonlinear viscoelastic regions. *Journal of Food Engineering, 121*, 58–63.
Liu, H., Xu, X. M., & Guo, S. D. (2007). Rheological, texture and sensory properties of low-fat mayonnaise with different fat mimetics. *LWT - Food Science and Technology, 40*(6), 946–954.
Lopes-da-Silva, J. A., & Monteiro, S. R. (2019). Gelling and emulsifying properties of soy protein hydrolysates in the presence of a neutral polysaccharide. *Food Chemistry, 294*, 216–223.
McClements, D. J. (2006). Non-covalent interactions between proteins and polysaccharides. *Biotechnology Advances, 24*(6), 621–625.
Navidghasemizad, S., Temelli, F., & Wu, J. (2014). Physicochemical properties of leftover egg yolk after livetins removal. *Food Science & Technology, 55*(1), 170–175.
Navidghasemizad, S., Temelli, F., & Wu, J. (2015). Phase separation behavior of egg yolk suspensions after anionic polysaccharides addition. *Carbohydrate Polymers, 117*, 297–303.
Necas, J., & Bartosikova, L. (2013). Carrageenan: a review. *Veterinarni Medicina, 58*(No. 4), 187–205.
Nguyen, B. T., Nicolai, T., Benyahia, L., & Chassenieux, C. (2014). Synergistic effects of mixed salt on the gelation of κ-carrageenan. *Carbohydrate Polymers, 112*, 10–15.
Nguyen, B. T., Nicolai, T., Chassenieux, C., & Benyahia, L. (2014). The effect of protein aggregate morphology on phase separation in mixtures with polysaccharides. *Journal of Physics: Condensed Matter, 26*(46), 464102.
Pereira, L., Sousa, A., Coelho, H., Amado, A. M., & Ribeiro-Claro, P. J. A. (2003). Use of FTIR, FT-Raman and ^{13}C-NMR spectroscopy for identification of some seaweed phycocolloids. *Biomolecular Engineering, 20*(4-6), 223–228.
Petruccelli, S., & Anon, M. C. (1995). Thermal aggregation of soy protein isolates. *Journal of Agricultural and Food Chemistry, 43*(12), 3035–3041.
Razzak, M. A., Kim, M., & Chung, D. (2016). Elucidation of aqueous interactions between fish gelatin and sodium alginate. *Carbohydrate Polymers, 148*, 181–188.
Samant, S., Singhal, R., Kulkarni, P., & Rege, D. (1993). Protein-polysaccharide interactions: A new approach in food formulations. *International Journal of Food Science & Technology, 28*(6), 547–562.
Severa, L., Nedomová, S., & Buchar, J. (2010). Influence of storing time and temperature on the viscosity of an egg yolk. *Journal of Food Engineering, 96*(2), 266–269.
Slade, L., Kweon, M., & Levine, H. (2021). Exploration of the functionality of sugars in cake-baking, and effects on cake quality. *Critical Reviews in Food Science and Nutrition, 61*(2), 283–311.
Sow, L. C., Nicole Chong, J. M., Liao, Q. X., & Yang, H. (2018). Effects of κ-carrageenan on the structure and rheological properties of fish gelatin. *Journal of Food Engineering, 239*, 92–103.
Takahashi, M., Ishmael, M., Asikin, Y., Hirose, N., Mizu, M., Shikanai, T., … Wada, K. (2016). Composition, taste, aroma, and antioxidant activity of solidified noncentrifugal brown sugars prepared from whole stalk and separated pith of sugarcane (*Saccharum officinarum L.*). *Journal of Food Science, 81*(11), C2647–C2655.
Takahashi, K., Kurose, K., Okazaki, E., & Osako, K. (2016). Effect of various protease inhibitors on heat-induced myofibrillar protein degradation and gel-forming ability of red tilefish (*Branchiostegus japonicus*) meat. *LWT - Food Science and Technology, 68*, 717–723.
Woodward, S. A., & Cotterill, O. J. (1987). Texture profile analysis, expressed serum, and microstructure of heat-formed egg yolk gels. *Journal of Food Science, 52*(1), 68–74.
Wu, D., Lin, Q., Singh, H., & Ye, A. (2020). Complexation between whey protein and octenyl succinic anhydride (OSA)-modified starch: Formation and characteristics of soluble complexes. *Food Research International, 136*, 109350.
Yang, D., Gao, S., & Yang, H. (2020). Effects of sucrose addition on the rheology and structure of iota-carrageenan. *Food Hydrocolloids, 99*, 105317.
Yang, Y., Zhao, Y., Xu, M., Yao, Y., Wu, N.a., Du, H., & Tu, Y. (2020). Effects of strong alkali treatment on the physicochemical properties, microstructure, protein structures, and intermolecular forces in egg yolks, plasma, and granules. *Food Chemistry, 311*, 125998.
Zhang, M., Li, J., Chang, C., Wang, C., Li, X., Su, Y., & Yang, Y. (2019). Effect of egg yolk on the textural, rheology and structural properties of egg gels. *Journal of Food Engineering, 246*, 1–6.
Zhou, M., Hu, Q., Wang, T., Xue, J., & Luo, Y. (2016). Effects of different polysaccharides on the formation of egg yolk LDL complex nanogels for nutrient delivery. *Carbohydrate Polymers, 153*, 336–344.